e-Navi

Available online at http://www.e-navigation.kr/
e-Navigation Journal

Original article

Adaptive Control with Time-Varying Disturbance Observation and Saturation Compensation under Phased Error Constraints

LI Xinyi[a*], LI Weihong[b], TAO Yuwen[c]

[a*]School of Navigation and Shipping, Shandong Jiaotong University, China, 13015950887@163.com

[b]School of Navigation and Shipping, Shandong Jiaotong University, China, 15964513537@163.com

[c]School of Navigation and Shipping, Shandong Jiaotong University, China, 1104699791@qq.com

Abstract

This paper investigates the problem of ship course control in the presence of model uncertainties, external disturbances, and actuator saturation. A high-performance autopilot is developed based on a direct neural network adaptive dynamic surface control (DSC) framework integrated with deep reinforcement learning. To compensate for lumped uncertainties arising from unmodeled dynamics and disturbances, a radial basis function (RBF) neural network is employed to provide online approximation within the control design. Moreover, the actuator saturation constraint is explicitly incorporated into the controller, avoiding performance degradation commonly encountered in conventional DSC schemes.To alleviate the reliance on manual parameter tuning, the controller parameter adaptation is formulated as a continuous-action optimization problem and solved using a deep deterministic policy gradient (DDPG) algorithm. The DDPG agent learns an optimal tuning policy by maximizing a reward function that penalizes course tracking errors, excessive control variations, and energy consumption. Simulation results demonstrate that the proposed method achieves improved tracking accuracy, smoother control inputs, and enhanced robustness under complex operating conditions, thereby validating the effectiveness of the DDPG-based adaptive tuning strategy for autonomous ship navigation.

Keywords: Ship Heading Control; Deep Deterministic Policy Gradient; Input Saturation; Dynamic Surface Control; Neural Network

https://doi.org/10.52820/j.enavi.2025.25.056

1. Introduction

Robust control of nonlinear systems under complex conditions such as unknown dynamics, time-varying disturbances, and actuator saturation is a current research hotspot in the field of control. Among traditional control methods, the Proportion Integration Differentiation (PID) controller (Zhao C, 2025) is widely used due to its simple structure, but its adaptability is insufficient in nonlinear time varying systems (Mccue L, 2016). Although sliding mode control (SMC) enhances anti-interference capability through switching terms (Liu S and Li P, 2019), high-frequency chattering can easily exacerbate actuator wear (ABY, 2018). To overcome model uncertainty, radial basis function neural networks (RBFNN) have been introduced in to adaptive control frameworks. For example, Chen C et al. (2017) uses RBFNN to approximate the nonlinear hydrodynamics of ships, but it does not consider input saturation constraints. Li K and Li Y (2020) further combines dynamic surface control (DSC) to alleviate the "curse of dimensionality" problem, but the control update frequency is still relatively high, making it difficult to meet the requirements of resource-constrained scenarios.

In the field of disturbance compensation, the latest advances in adaptive disturbance observers (ADO) and extended state observers (ESO) have provided new ideas for time-varying disturbance estimation. Wang J et al. (2024) proposes a composite disturbance observer that integrates neural networks and linear filters to improve estimation robustness in noisy environments. Chen W H et al. (2016) further designs an observer driven by deep reinforcement learning to enhance the generalization ability of dynamic disturbances, but it does not coordinate optimization of control efficiency. Dynamic threshold strategies reduce control update frequency and have shown significant advantages in robots (Qiu J, 2016) and unmanned aerial vehicles (Chen Q, 2016). For example, Yang X et al. (2022) proposes an adaptive threshold, but its parameter adaptability in the transient-steady state stage still needs to be improved.

Regarding input saturation problems, hard saturation strategies (Madeira D D S, 2024) are prone to stability risks, while Ge Q et al. (2025) proposes a continuous differentiable saturation function based on the Gaussian error function, which effectively suppresses high-frequency chattering. Xia X et al. (2024) combines an auxiliary dynamic system to compensate for saturation errors online, but it does not solve the dynamic performance optimization under asymmetric constraints. Phased control strategies balance convergence speed and steady-state accuracy through time-varying parameter adjustment. Sun Z Y et al. (2024) verifies the effectiveness of phased error constraints, but its theoretical framework in general nonlinear systems is not yet perfect.

Existing research faces three limitations: no systematic solution for suppressing coupled time-varying disturbances, input saturation, and Gaussian noise; an imperfect balance between control accuracy and computational efficiency; and fixed threshold strategies failing to meet the dual requirements of fast transient convergence and high steady-state precision in ship heading control.

Asymmetric input saturation, resulting from ship rudder physical limitations, hydrodynamic effects, and safety requirements, degrades performance when simplified to a symmetric model. To address this, this study sets the rudder angle saturation limit to [-10°, 15°] to align with maritime practice and enhance robust performance across all working conditions.

Aiming at the robust control problem of nonlinear systems under the coupled effects of time-varying disturbances, input saturation, and Gaussian noise, this paper proposes an adaptive control method integrating phased error constraints and asymmetric saturation compensation. By designing a time-varying disturbance observer to estimate disturbances online, combining the Gaussian error function to construct a continuous differentiable saturation model to handle asymmetric input constraints, and incorporating the noise upper bound into the sliding mode switching term design; innovatively using the phased error constraint strategy to dynamically adjust the error boundary; constructing a composite Lyapunov function at the theoretical level to prove that all signals of the closed-loop system are semi-globally uniformly ultimately bounded and the tracking error converges to a preset neighborhood.

2. Problem Analysis

2.1. Mathematical Model of the Ship Heading Control System

Consider an nth-order control system model with nonlinear uncertainties, unknown external disturbances, and time-varying disturbances:

$$\begin{aligned} \dot{x}_i &= f_i(\bar{\boldsymbol{x}}_i) + x_{i+1} + d_i(t) + \xi_i(t) \\ \dot{x}_n &= f_n(\bar{\boldsymbol{x}}_n) + g_n(\bar{\boldsymbol{x}}_n)u + d_n(t) + \xi_n(t) \\ y &= x_1 \end{aligned} \tag{1}$$

where $i = 1, \cdots, n-1$ and $x_i \in \{x_1, x_2, \cdots, x_n\}$ are the i-th system state variables, $i \in \{1, 2, \ldots, \mathrm{n}\}$, $\dot{x}_i$,

and $\dot{x}_n$ are the derivatives of the system state variables, $\bar{\boldsymbol{x}}_i$ is the vector of the first i states, and $\bar{\boldsymbol{x}}_n$ is the vector of n statesm. $f_i(\bar{\boldsymbol{x}}_i)$ is an unknown nonlinear function. $g_i(\bar{\boldsymbol{x}}_i), i=1,\cdots,n$ is a known control gain function, and $g_{\max} \geq |g_i(\bar{\boldsymbol{x}}_i)| \geq g_{\min} > 0$ ($g_{\min}$ and $g_{\max}$ are known positive constants). u is the control input; $d_i(t)$ is the i-th time-varying bounded disturbance, and it satisfies $\|d_i(t)\| \leq D$, (D is a known positive constant). $\xi_i(t) \square \square (0, \sigma_{\mathrm{n}}^2)$ is the i-th Gaussian noise. $u \in [u_{\min}, u_{\max}]$ represents the input saturation constraint. And y is the system output.

The following assumptions are made for the above system:

Assumption 1 The reference signal $y_d(t)$ is smooth and bounded, and has continuous bounded derivatives up to the n-th order, i.e, there exists a positive constant B such that the set $\{y_d(t), \dot{y}_d(t), \cdots, y_d^{(n)}(t), |y_d(t)| \leq B, |\dot{y}_d(t)| \leq B, |y_d^{(n)}(t)| \leq B\}$ holds (Wu S and Li X, 2024).

Assumption 2 The uncertainties $f_i(x_i)$ and the time-varying disturbance observer $d_i(t)$ have an upper bound, i.e, there exist unknown positive constants $d_i(t)$ and $\bar{d}$ such that $|f_i(\bar{\boldsymbol{x}}_i)| \leq \bar{f}$ and $|d_i(t)| \leq \bar{d}$ hold (Wu S and Li X, 2024) (Liu G,2024).

Assumption 3 $f_i(x_i)$ is an unknown nonlinear smooth function, whose derivative is known, and there exists a constant L_f such that $|f_i(x_1) - f_i(x_2)| \leq L_f \|x_1 - x_2\|$ holds; there exists a constant m_f such that $m_f \leq f_i(x_i) \leq -m_f$ holds (without loss of generality, assume $f_i(x_i)$ is bounded and its sign is known) (Liu G,2024).

Assumption 4 The time-varying disturbance $d_i(t)$ is continuously differentiable, and its derivative $\dot{d}_i(t)$ is bounded, i.e, there exists a positive constant M such that $\|\dot{d}_i(t)\| \leq M$ holds (Wu S and Li X, 2024) (Liu G,2024), which reflects the smoothness and finite energy of the actual disturbance. In practical applications, the original disturbance signal can be preprocessed through a low-pass filter to satisfy this assumption.

Assumption 5 Observer stability condition: There exists a positive constant $l_{i1}, l_{i2}, \sigma_{o,i}$ such that the observer gain satisfies $k_i > \frac{3}{2} + \frac{1}{2}\bar{g}_i^2$, $l_{i1} > \frac{3}{2} + \frac{1}{2}\bar{l}_i^2$, $\sigma_{di} > \frac{1}{2}$, $\sigma_i > \|\boldsymbol{\phi}_i\|^2$, $\sigma_{o,i} > \|\boldsymbol{\phi}_i\|^2$.

Design Objective: For the n th-order control system (1) with unknown nonlinear functions, unknown external disturbances, and a time-varying disturbance observer, in the presence of input saturation, a direct adaptive neural network controller is designed using Backstepping adaptive technology, DSC technology, neural network technology, and a saturation auxiliary design system. This controller ensures that all signals in the closed-loop system are semi-globally uniformly ultimately bounded, and the tracking error $z_1 = x_1 - y_{\mathrm{d}}$ can be made arbitrarily small. Meanwhile, a state observer for time-varying disturbances is designed to estimate the disturbances and improve control accuracy (Liu Jinhua, 2025) (Ning Jun, 2024).

2.2 Design of a Nonlinear Time-Varying Disturbance Observer

The nonlinear time-varying disturbance observer unifies nonlinear dynamic estimation and disturbance estimation in an extended state space by combining neural network approximation with dynamic compensation (Wu S and Li X, 2024), (Garone E, 2017) aiming to solve the state and disturbance estimation problem in system (1).

Step 1: State Observer Design

First a model-based state observer is designed to estimate the system states that cannot be directly measured:

$$\begin{aligned} \dot{\hat{\boldsymbol{x}}}_i &= \hat{\boldsymbol{W}}_{o,i}^T \boldsymbol{\phi}_i(\bar{\hat{\boldsymbol{x}}}_i) + g_i(\bar{\hat{\boldsymbol{x}}}_i)\hat{x}_{i+1} + \hat{\boldsymbol{d}}_i(t) + l_{i,1}(y - \hat{y}) \\ \dot{\hat{\boldsymbol{x}}}_n &= \hat{\boldsymbol{W}}_{o,n}^T \boldsymbol{\phi}_n(\bar{\hat{\boldsymbol{x}}}_n) + g_n(\hat{\boldsymbol{x}}_n)u + \hat{\boldsymbol{d}}_n(t) + l_{n,1}(y - \hat{y}) \end{aligned} \tag{2}$$

where $\hat{\boldsymbol{x}}_i$ denotes the estimated value of the i-t h state; $l_{i,1}$ and $l_{n,1}$ are the state observer gains; $g_i(\bar{\hat{\boldsymbol{x}}}_i)$ is a known control gain function; u is t he system control input vector; $\hat{\boldsymbol{W}}_{o,i}^T \boldsymbol{\phi}_i(\bar{\hat{x}}_i)$ is the approximation of the unknown nonlinear smooth function $f_i(\bar{\boldsymbol{x}}_i)$ by a radial basis function neural network; y is the measured value of the system actual output; $\hat{y}$ is the estimated value of the sy stem output; $\hat{\boldsymbol{d}}_i(t) = [\hat{d}_1(t), \hat{d}_2(t), \ldots, \hat{d}_n(t)]^T$ is the estimated value of the i-th time-varying disturba nce; and $\dot{\hat{\boldsymbol{d}}}_i(t) = [\dot{\hat{d}}_1(t), \dot{\hat{d}}_2(t), \ldots, \dot{\hat{d}}_i(t)]^T$ is the der ivative of the time-varying disturbance estimated value. This observer drives the state estimated va lue $y - \hat{y}$ to approach the true state $\boldsymbol{x}$ by using

the system model and the output error $\hat{\boldsymbol{x}}$.

Step 2: Disturbance Observer Design

Based on the obtained state estimate $\hat{\boldsymbol{x}}$, a distu rbance observer is designed to online estimate th e time-varying disturbance $\boldsymbol{d}_i(t)$. The dynamic d esign of the disturbance observer is as follows:

$$\dot{\hat{\boldsymbol{d}}}_i(t) = l_{i,2}(y - \hat{y}) - \sigma_i \hat{\boldsymbol{d}}_i(t) \tag{3}$$

In practice, the true state derivative $\dot{x}_i$ is unavail able and can be replaced using Equation (1) or obtained by designing a sliding mode differentiat or or other methods. Here, $\hat{\boldsymbol{d}}_i(t)$ denotes the est imated value of the i-th time-varying disturbance, $l_{i,2}$ is the disturbance observer gain, and σ_i is t he attenuation coefficient for disturbance estimati on. This design uses the differential signal of the state estimation error as the driving force, and en sures that $\hat{\boldsymbol{d}}_i(t)$ tracks the true disturbance $\boldsymbol{d}_i(t)$ through the gain $L_{d,i}$ and the attenuation dynami cs $-\sigma_i \hat{\boldsymbol{d}}_i(t)$.

As described above, the composite observer con sists core of the state observer (2) and the distur bance observer (3).

To analyze the stability of the state observer (2) and the disturbance observer (3), the state estimat ion error $\boldsymbol{e}_{o,i} = \boldsymbol{x}_i - \hat{\boldsymbol{x}}_i$ and the disturbance estima tion error $\boldsymbol{e}_{d,i} = \boldsymbol{d}_i(t) - \hat{\boldsymbol{d}}_i(t)$ are defined.

2.3. Asymmetric Saturation and Compensation by an Auxiliary Dynamic System

2.3.1 Asymmetric Saturation Model

Asymmetric saturation control is designed for sce narios where the actuator input has different amp litude limits in positive and negative directions, a iming to avoid the stability problems caused by hard saturation (Tran T, 2015) (Du H, 2016). Fo r the asymmetric saturation model, the saturation characteristic of the actuator input is defined as:

$$u_{\mathrm{p}} = sat(u_s) = \begin{cases} u_{\max}, & u_{\mathrm{s}} \geq u_{\max} \\ u_{\mathrm{s}}, & u_{\min} < u_{\mathrm{s}} < u_{\max} \\ u_{\min}, & u_{\mathrm{s}} \leq u_{\min} \end{cases} \tag{4}$$

where u_{s} is the original output command of the controller, u_{p} is the actual output control quantit y of the actuator, $u_{\max}$ is the positive saturation limit, $u_{\min}$ is the negative saturation limit, and $u_{\max} \neq |u_{\min}|$.

To avoid the control signal discontinuity and stab ility problems caused by hard saturation, a contin uous and differentiable saturation approximation model is constructed using the Gaussian error fu nction for smoothing (Su Wenxue, 2024) (Liu T, 2015):

$$\begin{aligned} u_t &= sat_{smooth}(u) \\ &= \frac{u_{\max} + u_{\min}}{2} + \frac{u_{\max} - u_{\min}}{2} \cdot erf\left(\frac{u_s - u_c}{\sigma}\right) \end{aligned} \tag{5}$$

where u_{c} is the saturation center, $\sigma > 0$ is the smoothing factor that controls the steepness of th e transition region. This smoothing model $sat_{smooth}(u)$ is used to characterize the saturation characteristic in theoretical analysis, while the co ntroller is designed based on the original comma nd u.

2.3.2 Auxiliary Dynamic System Compensation

To counteract the adverse effects of saturation no nlinearity on system stability, the following auxili ary dynamic system is introduced to generate the compensation signal:

$$\dot{\xi} = -k_{\xi}\xi + \Delta u \tag{6}$$

where ξ is the state variable of the auxiliary sy stem; $k_{\xi} > 0$ is the damping coefficient that ensu res the stability of the auxiliary system; $\Delta u = u_s - u_m$ is the control input difference caus ed by saturation. The output ξ of this auxiliary system will be integrated into the subsequent bac kstepping control design. Specifically, we will m odify the definition of the tracking error or the v irtual control law and introduce ξ as a compensa tion term.

Introducing auxiliary dynamic system compensatio n for saturation error $\Delta u_{\mathrm{a}} = u_{\mathrm{t}} - u_{\mathrm{s}}$:

$$\dot{e}_{\mathrm{c}} = -k_{\mathrm{d}} e_{\mathrm{c}} - \left|e_{\mathrm{c}} \Delta u_{\mathrm{a}}\right| + \gamma \Delta u_{\mathrm{a}} \tag{7}$$

where $k_{\mathrm{d}} > 0$ is the damping coefficient, e_{c} is t he state variable of the compensator, $\dot{e}_{\mathrm{c}}$ is the deriva tive of the state variable of the compensator, and $\gamma > 0$ is the coupling gain that ensures the boun dedness of e_{c} and suppresses the saturation effec t.

Combined with backstepping and asymmetric satu ration compensation, the control input is designed (Su Wenxue, 2024) (Jiao Jianfang, 2025):

$$\boldsymbol{v} = \boldsymbol{u}_{\mathrm{w}} + \boldsymbol{u}_{\mathrm{e}} \tag{8}$$

where $\boldsymbol{v}$ is the total control input; the equivalent control term $\boldsymbol{u}_{\mathrm{e}}$, designed based on the nominal model, such as sliding mode equivalent control;

Switching Control Term $\boldsymbol{u}_{\mathrm{w}}$:

$$\begin{aligned} \boldsymbol{u}_{\mathrm{w}} &= -K \cdot \mathrm{sat}\left(\frac{\boldsymbol{s}(t)}{\phi}\right) \\ &= -K \cdot \mathrm{sign}(\boldsymbol{s}(t)) \cdot \tanh\left(\frac{|\boldsymbol{s}(t)|}{\phi}\right) \end{aligned} \tag{9}$$

where $K>0$ is the compensation gain; $s_i(t)=\lambda_{\mathrm{s}} e_{\mathrm{s}}(t)+\dot{e}_{\mathrm{s}}(t)$ is the sliding mode surface variable, $\boldsymbol{s}(t)=[s_1(t),s_2(t),\ldots,s_i(t),\ldots,s_n(t)]^{\mathrm{T}}$; $\lambda_{\mathrm{s}}>0$ is the convergence rate parameter; $e_{\mathrm{s}}(t)$ is the basic tracking error, $\dot{e}_{\mathrm{s}}(t)$ is the derivative of the tracking error; $\phi>0$ is the smoothing par ameter that controls the slope of the transition re gion of the saturation function; $\mathrm{sat}(\cdot)$ is the smo othed saturation function, defined here as a hyper bolic tangent form; $\mathrm{sign}(\cdot)$ is the sign function; $\tanh(\cdot)$ is the hyperbolic tangent smoothing funct ion to avoid high-frequency switching.

2.4. Phase-by-Phase Error Constraints

Phase-by-phase error constraints adjust dynamic p erformance through time-varying parameters to ad apt to the requirements of different control phase s (Chen H, 2021). The error bounds are designed as follows:

$$E_{\mathrm{mi}}(t)=\begin{cases} E_{\mathrm{i}}, & t<T_3 \\ E_{\mathrm{m}}, & T_3 \le t < T_4 \\ E_{\mathrm{f}}, & t \ge T_4 \end{cases} \tag{10}$$

where $E_{\mathrm{mi}}(t)$ is the time-varying error bound; E_{i} is the initial phase boundary value; E_{m} is th e transition phase boundary value; E_{f} is the stea dy-state phase boundary value; T_3 and T_4 are th e phase switching time thresholds.

3. Controller Design and Stability Analysis

3.1. Controller Design

The tracking error is:

$$z_i=\begin{cases} \hat{x}_i - y_d, & i=1 \\ \hat{x}_i - a_{i\text{-}1}, & i=2,3,\ldots,n \end{cases} \tag{11}$$

where z_i is the i-th layer tracking error; $a_{i\text{-}1}$ is the i-th virtual control law. When $i=1$, $z_1=\hat{x}_1-y_d$ is the basic tracking error; when $i\ge 2$, $z_i=\hat{x}_i-a_{i\text{-}1}$ is the backstepping recursive error.

The sliding mode surface with error function (Du H, 2016) (Liu G,2024) is:

$$s_i(t)=\sum_{i=1}^{n}\lambda_i z_i+\sum_{i=1}^{n-1} a_i \cdot \mathrm{erf}\left(\frac{z_i}{a_i}\right) \tag{12}$$

where $s_i(t)\in\{s_1(t),s_2(t),\ldots,s_n(t)\}$ is the compos ite sliding mode surface; $\lambda_i>0$ is the convergen ce rate parameter of the i-th sliding mode surfac e, ensuring dynamic convergence speed; $\mathrm{erf}\left(\frac{z_i}{b_i}\right)=\frac{2}{\sqrt{\pi}}\int_0^{\frac{z_i}{b_i}} \mathrm{e}^{-t^2}dt$ is used to smooth the con trol law, e is the natural constant, and $b_i>0$ is the smoothing parameter of the i-th Gaussian err or function.

The sliding mode surface constraint is $|z_i|\le E_{\mathrm{mi}}(t), |s_i(t)|\le \sum_{i=1}^{n}\lambda_i E_{\mathrm{mi}}(t)$.

For the n-th order system (1), combined with t he neural network technology mentioned in Refer ence (Wu S and Li X, 2024), a design procedur e for direct adaptive neural network control consi dering system input saturation is proposed.

Step 1: Consider system (1) when $n=1$, define the first error surface $z_1=x_1-y_d(t)$, where $\dot{y}_d(t)$ is the derivative of the reference signal, a nd select the intermediate stabilizing function α_1 as the virtual control law for the first subsystem. Differentiating z_1 yields

$$\dot{z}_1=f_1(x_1)+x_2+\xi_1(t)+d_1(t)-\dot{y}_d \tag{13}$$

The virtual control law α_1 is selected as follow s:

$$\begin{aligned} \alpha_1=\frac{1}{g_1(\hat{x}_1)}[&-k_1 z_1+\dot{y}_d-\hat{d}_1(t) \\ &-\hat{W}_1^T\phi_1(\hat{x}_1)-l_{11}e_{o,1}] \end{aligned} \tag{14}$$

where $k_1 > 0$ is the error feedback gain parameter, the weight update law is:

$$\dot{\boldsymbol{W}}_1 = \gamma_1(\boldsymbol{S}_1(\boldsymbol{x}_1)z_1 - \sigma_1\boldsymbol{W}_1) \tag{15}$$

where $\boldsymbol{W}_1$ is the neural network weight vector, $\dot{\boldsymbol{W}}_1$ is the derivative of the neural network weight vector; γ_1 is the adaptive learning rate; $\boldsymbol{S}_1(\boldsymbol{x}_1)$ is the RBF basis function vector; $\sigma_1 > 0$ is the σ-correction coefficient.

[Note] The introduction of the correction term $\sigma_1\hat{\theta}_1$ for σ_1 is to improve the robustness of the neural network approximation error. Without this correction term, the neural network weight estimate $\hat{\theta}_1$ may drift to very large values, transforming it into a high-gain control algorithm (Wu S and Li X, 2024).

To avoid the problem of "computational explosion", α_1 is passed through a first-order filter ω_1 with a time constant τ_1 (Wu S and Li X, 2024), i.e.,

$$\tau_1\dot{\omega}_1 + \omega_1 = \alpha_1, \quad \omega_1(0) = \alpha_1(0) \tag{16}$$

where τ_1 is the filter time constant; ω_1 is the filtered virtual control signal, and $\dot{\omega}_1$ is the derivative of the filtered virtual control signal.

Define the second error surface $z_2 = x_2 - \omega_1$.

Step i: Consider system (1) when $1 < i < n$, similarly, consider $\dot{z}_i$, differentiating z_i yields

$$\dot{z}_i = f_i(\bar{\boldsymbol{x}}_i) + x_{i+1} + \xi_i(t) + d_i(t) - \dot{\omega}_{i-1} \tag{17}$$

The virtual control law α_{n-1} is selected as follows:

$$\begin{aligned}\alpha_i = \frac{1}{g_i(\bar{\hat{x}}_i)}[&-k_i z_i - \hat{\boldsymbol{W}}_i^T\boldsymbol{\phi}_i(\bar{\hat{x}}_i) - \hat{d}_i(t) \\ &-\dot{\alpha}_{i-1} - g_{i-1}z_{i-1} - l_{i1}e_{o,1}]\end{aligned} \tag{18}$$

where $k_i > 0$ is the i-th error feedback gain parameter.

Let α_i pass through a first-order filter ω_i with a time constant τ_i, i.e.,

$$\tau_i\dot{\omega}_i + \omega_i = \alpha_i, \quad \omega_i(0) = \alpha_i(0) \tag{19}$$

Step n: Define the n-th error surface $z_{i+1} = x_{i+1} - \omega_i$ (Wu S and Li X, 2024). Considering $\dot{z}_n$, differentiating z_n yields:

$$\dot{z}_n = f_n(\bar{\boldsymbol{x}}_n) + g_n(\bar{\boldsymbol{x}}_n)u + \xi_n(t) + d_n(t) - \dot{\omega}_{n-1} \tag{20}$$

Gaussian noise compensation, the variance σ_n^2 of the noise term $\xi_i(t)$ adjusts the noise intensity through the standard deviation. Assuming bounded noise satisfies $|\xi_i(t)| \le \bar{\xi}_i$, and incorporates it into the disturbance term in the Lyapunov function analysis.

Input saturation is smoothed using a Gaussian error function (Chen H, 2021):

$$u_t = u_c + f \cdot \mathrm{erf}(\sqrt{\pi} \cdot \frac{u_s - u_c}{f}) \tag{21}$$

The saturation error $\Delta u_a = u_t - u_s$ is compensated by an auxiliary system.

To conveniently consider the effect of system input saturation $u = \mathrm{sat}(v)$, the auxiliary design system is selected as follows:

$$\begin{aligned}\dot{\boldsymbol{y}}_e = &-\frac{\left(\sum_{i=1}^{n}|z_i(u_t - \boldsymbol{v})| + \eta(u_t - \boldsymbol{v})^2\right)}{\boldsymbol{y}_e} \\ &-k_e\boldsymbol{y}_e + \Delta u_a\end{aligned} \tag{22}$$

The equivalent control term $\boldsymbol{u}_e$ is as follows (Chen H, 2021):

$$\begin{aligned}\boldsymbol{u}_e = \frac{1}{g_n(\bar{\hat{x}}_n)}[&(-k_n z_n - \hat{\boldsymbol{W}}_n^T\boldsymbol{\phi}_n(\bar{\hat{x}}_n) - \hat{d}_n \\ &+\dot{\alpha}_{n-1} - g_{n-1}z_{n-1} - l_{n1}e_{o,1}]\end{aligned} \tag{23}$$

where $g_n(\bar{\hat{x}}_n)$ is the known control gain estimate; k_n is a positive definite control gain ($k_n > 0$); $g_{n-1}z_{n-1}$ is a stability compensation term used to cancel the influence of the error dynamics from the previous step.

The switching control term $\boldsymbol{u}_w$ adopts a saturation function to reduce high-frequency chattering (Chen H, 2021), as follows:

$$\boldsymbol{u}_w = -\frac{1}{g_n(x_n)}\hat{\rho}_n \cdot sat(\frac{z_n}{\phi}) \tag{24}$$

The total control rate is:

$$\boldsymbol{v} = \boldsymbol{u}_{\mathrm{e}} + \boldsymbol{u}_{\mathrm{w}} \tag{25}$$

3.2. Nonlinear Time-Varying Disturbance Observer Design

Based on the nonlinear system model (1) in Se ction 2.1, the corresponding nonlinear time-varyin g disturbance observer is designed as follows

$$\begin{cases} \dot{\hat{\boldsymbol{x}}}_i = \hat{\boldsymbol{W}}_{o,i}^T \boldsymbol{\phi}_i(\hat{\boldsymbol{x}}_i) + g_i(\hat{\boldsymbol{x}}_i)\hat{x}_{i+1} + \hat{\boldsymbol{d}}_i(t) + l_{i1}(x_1 - \hat{x}_1) \\ \dot{\hat{\boldsymbol{x}}}_n = \hat{\boldsymbol{W}}_{o,n}^T \boldsymbol{\phi}_n(\bar{\hat{\boldsymbol{x}}}_n) + g_n(\bar{\hat{\boldsymbol{x}}}_n)u + \hat{\boldsymbol{d}}_n(t) + l_{n1}(x_1 - \hat{x}_1) \\ \dot{\hat{\boldsymbol{d}}}_i(t) = l_{i2}(x_1 - \hat{x}_1) - \sigma_{di}\hat{\boldsymbol{d}}_i(t) \\ \dot{\hat{\boldsymbol{d}}}_n(t) = l_{n2}(x_1 - \hat{x}_1) - \sigma_{dn}\hat{\boldsymbol{d}}_n(t) \end{cases} \tag{26}$$

where $\bar{\hat{\boldsymbol{x}}}_{\boldsymbol{i}}$ denotes the vector $\left[\hat{x}_1, \hat{x}_2, \ldots, \hat{x}_i\right]^T$; σ_{di} and σ_{dn} are the disturbance estimation attenuatio n parameters.

Define the observation error $e_{o,i} = x_i - \hat{x}_i$ and th e disturbance estimation error $e_{d,i} = d_i(t) - \hat{d}_i(t)$, the error dynamics can be obtained as:

$$\begin{cases} \dot{\boldsymbol{e}}_{\mathrm{o,i}} = e_{d,i} - l_{i1}e_{o,1i} + [f_i(\bar{\boldsymbol{x}}_i) - \hat{\boldsymbol{W}}_{o,i}^T \boldsymbol{\phi}_i(\bar{\hat{\boldsymbol{x}}}_i)] \\ \qquad + [g_i(\bar{\boldsymbol{x}}_{\boldsymbol{i}})x_{i+1} - g_i(\bar{\hat{\boldsymbol{x}}}_{\boldsymbol{i}})\hat{x}_{i+1}] + \xi \\ \dot{\boldsymbol{e}}_{\mathrm{o,n}} = e_{d,n} - l_{n1}e_{o,1} + [f_n(\bar{\boldsymbol{x}}_{\boldsymbol{n}}) - \hat{\boldsymbol{W}}_{o,n}^T \boldsymbol{\phi}_n(\bar{\hat{\boldsymbol{x}}}_n)] \\ \qquad + [g_n(\bar{\boldsymbol{x}}_n) - g_n(\bar{\hat{\boldsymbol{x}}}_n)]u + \xi_n \end{cases} \tag{27}$$

$$\begin{cases} \dot{\boldsymbol{e}}_{d,i} = \dot{\boldsymbol{d}}_i - l_{i2}\boldsymbol{e}_{o,1} + \sigma_{di}\hat{\boldsymbol{d}}_i \\ \dot{\boldsymbol{e}}_{d,n} = \dot{\boldsymbol{d}}_n - l_{n2}\boldsymbol{e}_{o,1} + \sigma_{dn}\hat{\boldsymbol{d}}_n \end{cases} \tag{28}$$

where x_{i+1} is the actual state, $\hat{x}_{i+1}$ is the estimat ed state; ξ_i and ξ_n are modeling errors or noise; $\dot{\boldsymbol{d}}_i$ and $\dot{\boldsymbol{d}}_n$ are the derivatives of the actual distu rbance.

$$\dot{\hat{\boldsymbol{W}}}_{o,i} = \boldsymbol{\Gamma}_{o,i}[\boldsymbol{\phi}_i(\bar{\hat{\boldsymbol{x}}}_i)\boldsymbol{e}_{o,i} - \sigma_{o,i}\hat{\boldsymbol{W}}_{o,i}], i = 1, \ldots, n \tag{29}$$

where $\dot{\hat{\boldsymbol{W}}}_i$ is the time derivative of the i-th wei ght estimation vector; $\boldsymbol{\Gamma}_{o,i}$ is a positive definite matrix, which is the observer neural network lear ning rate matrix; $\sigma_{o,i}$ is the σ-correction coeffic ient.

3.3. Stability Analysis

For the time-varying disturbance observer, constr uct a Lyapunov function including the observer e rror.

$$\begin{aligned} V = & \frac{1}{2}\sum_{i=1}^{n} z_i^2 + \frac{1}{2}\sum_{i=1}^{n} \eta_i^2 \\ & + \frac{1}{2}\sum_{i=1}^{n} \boldsymbol{e}_{o,i}^T \boldsymbol{P}\boldsymbol{e}_{o,i} + \frac{1}{2}\sum_{i=1}^{n} \boldsymbol{e}_{d,i}^T \boldsymbol{Q}\boldsymbol{e}_{d,i} \\ & + \frac{1}{2}\sum_{i=1}^{n} \tilde{\boldsymbol{W}}_i^{\mathrm{T}} \boldsymbol{\Gamma}_i^{-1} \tilde{\boldsymbol{W}}_i + \frac{1}{2}\sum_{i=1}^{n} \tilde{\boldsymbol{W}}_{\boldsymbol{o,i}}^{\boldsymbol{T}} \boldsymbol{\Gamma}_{\boldsymbol{o,i}}^{\boldsymbol{-1}} \tilde{\boldsymbol{W}}_{\boldsymbol{o.i}} \end{aligned} \tag{30}$$

where $\tilde{\boldsymbol{W}}_i = \boldsymbol{W}_i - \boldsymbol{W}_i^*$ is the controller neural net work weight error; $\tilde{\boldsymbol{W}}_{o,i} = \boldsymbol{W}_{o,i}^{\ *} - \hat{\boldsymbol{W}}_{o,i}$ is the obse rver neural network weight error; η_i is the robus t term parameter.

Differentiating V yields:

$$\begin{aligned} \dot{V} = & \sum_{i=1}^{n} \mathrm{z}_i \dot{\mathrm{z}}_i + \sum_{i=1}^{n} \boldsymbol{e}_{o,i}\boldsymbol{P}\dot{\boldsymbol{e}}_{o,i} + \sum_{i=1}^{n} \boldsymbol{e}_{d,i}\boldsymbol{Q}\dot{\boldsymbol{e}}_{d,i} \\ & - \sum_{i=1}^{n} \tilde{\boldsymbol{W}}_i^{\mathrm{T}} \boldsymbol{\Gamma}_i^{-1} \dot{\hat{\boldsymbol{W}}}_i - \sum_{i=1}^{n} \tilde{\boldsymbol{W}}_{o,i}^{\mathrm{T}} \boldsymbol{\Gamma}_{o,i}^{-1} \dot{\hat{\boldsymbol{W}}}_{o,i} + \sum_{i=1}^{n} \eta_i \dot{\eta}_i \end{aligned} \tag{31}$$

Expand term by term: Dynamic analysis of trac king error:

Step 1:

$$\begin{aligned} \dot{z}_1 = & -k_1 z_1 + (\tilde{\boldsymbol{W}}_{\boldsymbol{o,1}} - \tilde{\boldsymbol{W}}_{\boldsymbol{1}})^T \boldsymbol{\phi}_1(\hat{x}_1) \\ & + g_1(\hat{x}_1)z_2 - \eta_1 sat(\frac{z_1}{\varepsilon_1}) + \varepsilon_1 + \Delta g_1 \end{aligned} \tag{32}$$

where $\Delta g_1 = g_1(x_1)x_2 - g_1(\hat{x}_1)\hat{x}_2$ is the control ga i n e r r o r ; $\varepsilon_1 = \boldsymbol{W}_1^{*T}\boldsymbol{\phi}_1(x_1) - \hat{\boldsymbol{W}}_{o,1}^T \boldsymbol{\phi}_1(\hat{x}_1) = \boldsymbol{W}_1^{*T}(\boldsymbol{\phi}_1(x_1) - \boldsymbol{\phi}_1(\hat{x}_1))$ $+\tilde{\boldsymbol{W}}_{o,1}^T \boldsymbol{\phi}_1(\hat{x}_1)$ is the neural network approximation error.

Step i:

$$\begin{aligned} \dot{z}_i = & \dot{\hat{x}}_i - \dot{\alpha}_{i-1} \\ = & -k_i z_i + (\tilde{\boldsymbol{W}}_{\boldsymbol{o,i}} - \tilde{\boldsymbol{W}}_i)^T \phi_i(\bar{\hat{\boldsymbol{x}}}_i) + g_i(\bar{\hat{\boldsymbol{x}}}_i)z_{i+1} \\ & - g_{i-1}(\bar{\hat{\boldsymbol{x}}}_{i-1})z_{i-1} - \eta_i sat(\frac{z_i}{\varepsilon_i}) + \varepsilon_i + \Delta g_i \end{aligned} \tag{33}$$

Step n:

$$\begin{aligned} \dot{z}_n = & \dot{\hat{x}}_n - \dot{\alpha}_{n-1} \\ = & -k_n z_n + (\tilde{\boldsymbol{W}}_{o,n}^{\mathrm{T}} - \tilde{\boldsymbol{W}}_n)^T \phi_n(\bar{\hat{\boldsymbol{x}}}_n) - \eta_n sat(\frac{z_n}{\varepsilon_n}) \\ & - g_{n-1}(\bar{\hat{\boldsymbol{x}}}_{n-1})z_{n-1} - \rho_n \tanh(\frac{s_n}{\delta_n}) + \varepsilon_n + \Delta g_{\mathrm{n}} \end{aligned} \tag{34}$$

Observation Error Dynamic Analysis

$$\begin{aligned}\dot{\boldsymbol{e}}_{o,i} &= \dot{\boldsymbol{x}}_i - \dot{\hat{\boldsymbol{x}}}_i \\ &= [f_i(\bar{x}_i) + g_i(\bar{x}_i)x_{i+1} + \boldsymbol{d}_i(t) + \xi_i] \\ &\quad -[\hat{\boldsymbol{W}}_{o,i}^T \boldsymbol{\phi}_i(\bar{\hat{\boldsymbol{x}}}_i) + g_i(\bar{\hat{\boldsymbol{x}}}_i)\hat{x}_{i+1} + \hat{\boldsymbol{d}}_i(t) + l_{i1}\boldsymbol{e}_{o,1}] \\ &= -\tilde{\boldsymbol{W}}_{o,i}^T \boldsymbol{\phi}_i(\bar{\hat{\boldsymbol{x}}}_i) + \varepsilon_{o.i} + \Delta f_i \\ &\quad +\Delta g_{o,i} + \boldsymbol{e}_{d,i} - l_{i1}\boldsymbol{e}_{o,1} + \xi_i\end{aligned} \tag{35}$$

where $\varepsilon_{o.i} = f_i(\bar{x}_i) - \boldsymbol{W}_{o,i}^{*T}\phi_i(\bar{\hat{x}}_i)$ is the observer neural network approximation error; $\Delta f_i = \boldsymbol{W}_{o,i}^{*T}[\boldsymbol{\phi}_i(\bar{\hat{\boldsymbol{x}}}_i) - \boldsymbol{\phi}_i(\bar{\boldsymbol{x}}_i)]$ is the basis function error; $\Delta g_{o,i} = g_i(\bar{x}_i)x_{i+1} - g_i(\bar{\hat{\boldsymbol{x}}}_i)\hat{\boldsymbol{x}}_{i+1}$ is the observer control gain error.

$$\begin{aligned}\dot{V} \le & -\sum_{i=1}^{n}[k_i - \frac{3}{2} - \frac{1}{2}\bar{g}_i^2]z_i^2 \\ & -\sum_{i=1}^{n}[l_{i1} - \frac{3}{2} - \frac{1}{2}\bar{l}_i^2]\boldsymbol{e}_{o,i}^2 \\ & -\sum_{i=1}^{n}[\sigma_{di} - \frac{1}{2}]\boldsymbol{e}_{d,i}^2 \\ & -\sum_{i=1}^{n}[\frac{\sigma_i}{2} - \frac{1}{2}\|\boldsymbol{\phi}_i\|^2]\|\tilde{\boldsymbol{W}}_i\|^2 \\ & -\sum_{i=1}^{n}[\frac{\sigma_{o,i}}{2} - \frac{1}{2}\|\boldsymbol{\phi}_i\|^2]\|\tilde{\boldsymbol{W}}_{o,i}\|^2 \\ & -\sum_{i=1}^{n}\sigma_{\eta,i}\eta_i^2 + \Delta\end{aligned} \tag{36}$$

where $\Delta = \sum_{i=1}^{n}[\frac{1}{2}\bar{\varepsilon}_i^2 + \frac{1}{2}\bar{\varepsilon}_{o,i}^2 + \frac{1}{2}\bar{h}_i^2(t) + \frac{1}{2}\bar{\xi}_i^2 + \frac{\sigma_i}{2}\|\boldsymbol{W}_i^*\|^2 + \frac{\sigma_{o,i}}{2}\|\boldsymbol{W}_{o,i}^*\|^2]$ is the sum of all bounded terms.

The final boundedness conclusion $\dot{V} \le -cV + \Delta$, obtained by the comparison lemma, gives: $V(t) \le V(0)e^{-ct} + \frac{\Delta}{c}(1 - e^{-ct})$. Therefore, all signals are semi-globally uniformly ultimately bounded, and the tracking error, observation error, and estimation error converge to a compact set. Thus, it is proven that the system is stable under the combined action of the controller and observer, and can effectively improve the system's ability to estimate and compensate for disturbances, enhancing the control accuracy of the system under time-varying disturbances.

4. Simulation Verification

A simulation study is conducted using a specific training vessel as the application example. The vessel has a length L of 126.0 m, a beam B of 20.8 m, and a full-load draft d of 8.0 m (Wu S and Li X, 2024). The parameters $\mathrm{K} = 0.478$, $\mathrm{T} = 216$, $a_1 = 1, a_2 = 30$ of the ship's nonlinear motion mathematical model are calculated.

In the simulation, the initial conditions are selected as follows: the initial state of x_1 is 20°, the initial state of x_2 is zero, and the controller gains $\mathrm{k}_1 = 0.15$, $\mathrm{k}_2 = 120$, $\tau = 0.5$, $\gamma = 0.01$, $\sigma = 200$ as well as the observer gain matrix $\boldsymbol{L} = [2,1,5]^T$ are selected.

Computer simulation studies are carried out using MATLAB, and the results are as follows:

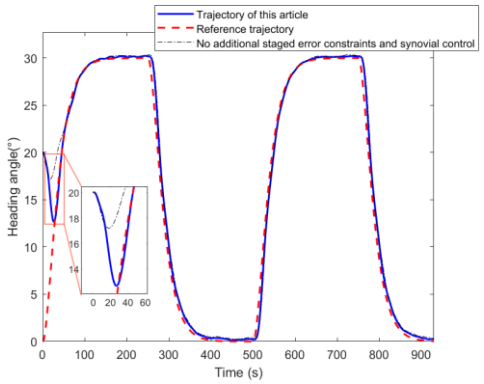

Fig. 1 Heading Tracking Comparison

Figure 1 is a course tracking comparison diagram. In the figure, the blue solid line represents the trajectory tracking situation of this paper, the black dashed line represents the tracking situation of the ship without the asymmetric saturation and sliding mode control, and the red dashed line represents the reference trajectory tracking situation. According to the image, the course of the red solid line can approach the actual situation of the ship faster than the blue dashed line and the black dashed line.

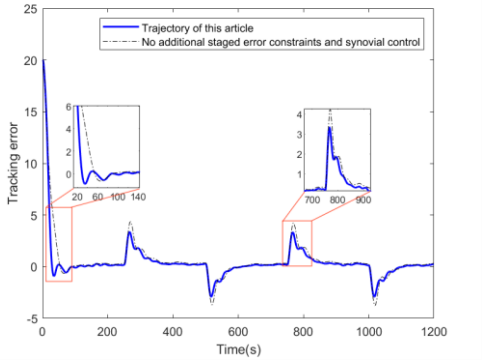

Fig. 2 Ship Tracking Error

In Figure 2, the blue solid line represents the f

unction of this paper, and the black dashed line represents the tracking situation of the ship witho ut sliding mode, asymmetric function unknown a daptation, and neural networks. By comparing the two curves, it can be concluded that the tracking error of the blue solid line shrinks faster and the error value is also smaller.

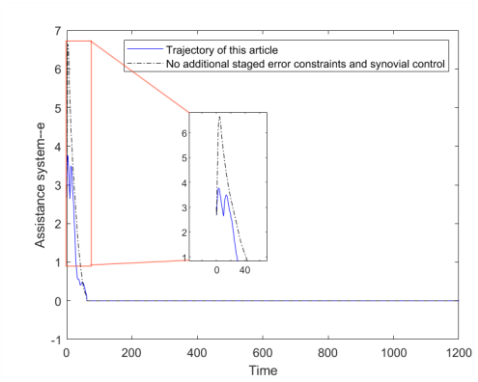

Fig. 3 Comparison of Dynamic Changes in Auxiliar y System State Variables

In Figure 3, the blue solid line represents the f unction of this paper, and the black dashed line represents the tracking situation of the ship witho ut sliding mode, asymmetric function unknown a daptation, and neural networks. By comparing the two curves, it can be concluded that the blue sol id line has a smaller range of variation in the au xiliary system variables.

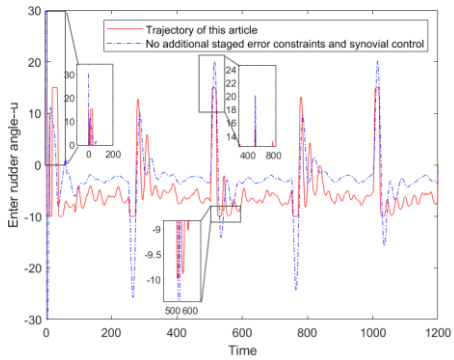

Fig. 4 Dynamic Variation of Input Rudder Angle u with and without Asymmetric Saturation Control

In Figure 4, the blue dashed line represents the dynamic variation of the input rudder angle u wi thout the asymmetric saturation control function, and the red solid line represents the dynamic var iation of the input rudder angle u with the asym metric saturation control function. By comparing the two curves in the figure, it can be clearly se en that the interval of the asymmetric saturation control function is between 15° and −10.

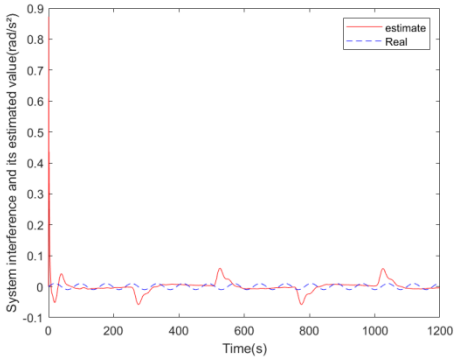

Fig. 5 Comparison of Time-Varying Observer Distu rbances with Their Estimated and Actual Values

In Figure 5, the red solid line represents the est imated value of the time-varying disturbance by t he time-varying disturbance observer, and the blu e dashed line represents the true value of the ti me-varying disturbance. By comparing the two c urves, it can be concluded that the time-varying disturbance estimated by the time-varying disturba nce observer has a large initial deviation, gradual ly becomes stable afterwards. Although there is s till oscillation, the overall amplitude is small.

5. Conclusion

This study addresses the robust control problem of complex nonlinear systems under multiple con straints, including unknown dynamics, time-varyin g disturbances, and input saturation. A dynamic s urface control technique is employed to suppress computational complexity, an improved radial basi s function neural network is combined to achieve efficient approximation of unknown dynamics, an d a phase-based error constraint strategy is desig ned to dynamically optimize the convergence spe ed and steady-state accuracy. For the asymmetric saturation issue, a compensation mechanism based on an auxiliary dynamic system is constructed, ef fectively balancing the actuator energy consumpti on and anti-high-frequency chattering performance. Simulation experiments using a ship course keepi ng control system verify the effectiveness of the proposed method. The asymmetric saturation com pensation strategy effectively suppresses the high-frequency chattering of the actuator and maintain s course stability in Gaussian noise environments. This study relies on the observability assumption of disturbance upper bounds and the persistent ex citation condition for neural network parameter c onvergence, which does not fully consider the im pact of communication delays and data packet lo ss, and is limited to the single-agent system scen ario. Future research can combine distributionally robust optimization with transfer learning to desig n an adaptive control architecture that does not d epend on prior disturbance information, integrate

time-delay compensation mechanisms and multi-agent coordination strategies, and develop methods for stable and convergent neural network parameters under low excitation conditions.

References

Zhao C, Wang D, Xue W.Beyond linear limits: Design of robust nonlinear PID control[J].Automatica, 2025, 173.

Mccue L.Handbook of Marine Craft Hydrodynamics and Motion Control[J].IEEE Control Systems, 2016, 36 (1):78-79.

Liu S, Li P.A novel chattering-free pi sliding mode control for a class of nonlinear underactuated systems[J]. International Journal of Modelling Identification and Control, 2019, 32(1):54.

ABY, BTY, A H S,et al.Robust sliding-mode control of wind energy conversion systems for optimal power extraction via nonlinear perturbation observers[J].Applied Energy, 2018, 210:711-723.

Chen C L P, Wen G X, Liu Y J, et al.Observer-Based Adaptive Backstepping Consensus Tracking Control for High-Order Nonlinear Semi-Strict-Feedback Multiagent Systems[J].IEEE Transactions on Cybernetics, 2017, 46(7):1591-1601.

Li K, Li Y. Adaptive Neural Network Finite-Time Dynamic Surface Control for Nonlinear Systems[J]. IEEE Transactions on Neural Networks and Learning Systems, 2020, PP(99):1-10.

Wang J, Wang D, Shen Y H. Composite Antidisturbance H∞ Control for Hidden Markov Jump Systems With Multi-Sensor Against Replay Attacks[J]. IEEE Transactions on Automatic Control, 2024, 69(3):1760-1766.

Chen W H, Yang J, Guo L,et al.Disturbance-Observer-Based Control and Related Methods—An Overview[J]. IEEE Transactions on Industrial Electronics, 2016, 63 (2):1083-1095.

Qiu J, Gao H, Ding S X.Recent Advances on Fuzzy-Model-Based Nonlinear Networked Control Systems: A Survey[J]. IEEE Transactions on Industrial Electronics, 2016, 63(2):1207-1217.

Chen Q, Liu G, Zhao W,et al.Asymmetrical SVPWM Fault-Tolerant Control of Five-Phase PM Brushless Motors[J]. IEEE Transactions on Energy Conversion, 2016, PP(1):1-1.

Yang X, Pan Y, Sun J,et al.Optimized adaptive event-triggered tracking control formulti-agent systems with full-state constraints[J]. International Journal of Robust and Nonlinear Control, 2022, 32:10101 - 10124.

Madeira D D S, Correia W B.Data-Driven Saturated State Feedback Design for Polynomial Systems Using Noisy Data[J]. IEEE Transactions on Automatic Control, 2024(11):69.

Ge Q, Bai X, Zeng P. Gaussian-Cauchy Mixture Kernel Function Based Maximum Correntropy Criterion Kalman Filter for Linear Non-Gaussian Systems[J]. IEEE Transactions on Signal Processing, 2025.

Xia X, Li C, Zhang T,et al.Finite-time optimal control for uncertain strict-feedback nonlinear systems with input saturation and output constraints[J]. International journal of adaptive control and signal processing, 2024 (2):38.

Sun Z Y, Li J J, Wen C,et al. Adaptive Event-Triggered Prescribed-Time Stabilization of Uncertain Nonlinear Systems With Asymmetric Time-Varying Output Constraint[J].IEEE Transactions on Automatic Control, 2024(8):69.

Wu S, Li X.Finite-Time Synchronization of Complex Dynamical Networks With Input Saturation[J].IEEE transactions on cybernetics, 2024, 54(1):364-372.

Garone E, Di Cairano S, Kolmanovsky I .Reference and command governors for systems with constraints: A survey on theory and applications[J].Automatica, 2017, 75:306-328.

Tran T, Ge S S, He W.Adaptive control for a robotic manipulator with uncertainties and input saturations[C]//IEEE International Conference on Mechatronics & Automation.IEEE, 2015.

Du H, Yu X, Chen M Z Q,et al.Chattering-free discrete-time sliding mode control[J]. Automatica, 2016, 68:87-91.

Su Wenxue, Meng Xiangfei, Zhang Qiang. Nonlinear Feedback Ship Heading Control Based on Adaptive RBF Neural Network Under Input Saturation Constraints [J]. Journal of Shanghai Maritime University,2024,45(02):14-19.

Liu T, Jiang Z P.A Small-Gain Approach to Robust Event-Triggered Control of Nonlinear Systems[J]. IEEE Transactions on Automatic Control, 2015, 60(8):1-1.

Jiao Jianfang, Bao Duanhua, Hu Zhengzhong. Neural Network Sliding Mode Control-Based Event-Triggered Prescribed Performance Tracking Control for Ships [J]. Control Engineering, 2025, 32(02):193-200.

Chen H, Liu Y J, Liu L,et al.Anti-Saturation-Based A daptive Sliding-Mode Control for Active Suspension S ystems With Time-Varying Vertical Displacement and Speed Constraints[J]. IEEE Transactions on Cybernetics, 2021, PP(99):1-11.

Liu G, Zhang Y, Hua C ,et al.Adaptive Fuzzy Trackin g Control for Nonlinear Time-Delay Systems With Per formance Constrained by Deferred Monotone Tube Bo undaries[J]. IEEE Transactions on Fuzzy Systems, 2024 (11):32.

Liu Jinhua, Wang Yuan, Zhang Zhixuan, et al. Robust Adaptive Backstepping Sliding Mode Control of Quad copter UAV Based on RBF Network[J]. Journal of Jia ngsu University (Natural Science Edition), 2025, 46(0 1):36-42.

Ning Jun, Liu Zihan, Li Wei, et al. Adaptive Quantiz ed Neural Network Sliding Mode Control for Unmann ed Surface Vehicle Formation [J]. Journal of Shanghai Maritime University, 2024, 45(02): 7-13.

Received **30 December 2025**

Accepted **05 January 2026**